ARTICLE OPEN

Check for updates

Medial prefrontal cortex Notch1 signalling mediates methamphetamine-induced psychosis via Hes1-dependent suppression of $GABA_{B1}$ receptor expression

Tong Ni[1,2], Li Zhu[1,2], Shuai Wang[1,2], Weili Zhu[3], Yanxue Xue[3], Yingjie Zhu[4,5], Dongliang Ma[6], Hongyan Wang[6,7], Fanglin Guan[1,2]✉ and Teng Chen[1,2]✉

Methamphetamine (METH), a widely abused stimulant drug, induces psychosis in approximately half of abusers; this effect is becoming a major concern for society. Although the Notch1 signalling pathway has been shown to play a part in the pathogenesis of some psychiatric disorders, its role in METH-induced psychosis (MIP) is still unknown. Here, the METH-induced locomotor sensitization model in rodents is considered to represent the underlying neurochemical changes driving psychoses. We found that the Notch1 signalling was downregulated in the medial prefrontal cortex (mPFC) in sensitized mice. Direct genetic and pharmacological manipulations of Notch1 signalling bidirectionally altered METH-induced locomotor sensitization and other MIP-related behaviours through governing neuronal activity in the mPFC. Moreover, Notch1 signalling negatively regulated $GABA_{B1}$ receptor expression in the mPFC of METH-sensitized mice through Hes1, a transcriptional repressor in Notch1 signalling. Further, we show that Hes1 can directly bind to the $GABA_{B1}$ receptor promoter. Notably, pharmacological regulation of the $GABA_B$ receptor in the mPFC reversed the changes in METH-induced locomotor sensitization caused by the dysfunction of Notch1 signalling. Together, our findings uncover a previously unrecognised Notch1-Hes1-$GABA_{B1}$ receptor-dependent mechanism involved in regulating mPFC neuronal activity and behavioural phenotypes in MIP. Our work provides mechanistic insight into the aetiology and pathophysiology of MIP.

Molecular Psychiatry (2022) 27:4009–4022; https://doi.org/10.1038/s41380-022-01662-z

INTRODUCTION

Methamphetamine (METH) is the second most common illicit drug worldwide, with 33 million users [1]. Apart from its strong addictive properties, one of the most widely known health consequences associated with high-dose or chronic METH use is METH-induced psychosis (MIP), which affects between 26 and 46% of people with a METH dependence [2, 3]. MIP displays symptoms similar to schizophrenia (SCZ) [4], including hyperactivity, agitation and cognitive deficiency, making it difficult to distinguish from SCZ clinically [5]. Despite the similarity between SCZ and MIP, the pathogenesis of MIP is different from SCZ and remains poorly understood.

Behavioural sensitization refers to the unique phenomenon whereby repeated exposure to a stimulus results in progressively increased behavioural activity in response to the stimulus following a period of abstinence [6]. Indeed, a single low-dose re-exposure to METH after decades of abstinence can cause MIP patients to display hyperactivity (manifested as hyperlocomotion) and a relapsed psychotic state [7, 8]. In animal studies, a METH-induced behavioural sensitization model also recapitulated MIP-related behaviours, including deficits in social behaviour [9], cognitive functions [10], and sensory gating [11], which mimic the symptoms observed in patients with MIP and can be ameliorated by antipsychotic drugs [12]. Psychosis-related proteins were also detected in the medial prefrontal cortex (mPFC) of sensitized mice by proteomics studies [13, 14]. Hence, the METH-induced behavioural sensitization model is the most relevant model of MIP thus far [15]. Understanding the mechanism of METH sensitization is important for determining the aetiology of MIP that is distinct from SCZ.

The highly conserved Notch signal pathway is involved in multiple crucial processes, including stem cell fate determination and diversification during development [16]. After the Notch receptor (Notch1-4) interacts with one of its ligands (Delta or Jagged), the Notch intracellular domain is released by γ-secretase-mediated cleavage and moves into the nucleus, where it initiates

[1]College of Forensic Medicine, Xi'an Jiaotong University Health Science Center, Xi'an, Shaanxi 710061, P R China. [2]The Key Laboratory of Health Ministry for Forensic Science, Xi'an Jiaotong University, Xi'an, Shaanxi 710061, P R China. [3]National Institute on Drug Dependence and Beijing Key Laboratory of Drug Dependence, Peking University, Beijing 100191, P R China. [4]Shenzhen Key Laboratory of Drug Addiction, CAS Key Laboratory of Brain Connectome and Manipulation, the Brain Cognition and Brain Disease Institute (BCBDI), Shenzhen Institutes of Advanced Technology, Chinese Academy of Sciences, Shenzhen 518055, P R China. [5]Shenzhen-Hong Kong Institute of Brain Science-Shenzhen Fundamental Research Institutions, Shenzhen 518055, P R China. [6]Programme in Neuroscience and Behavioral Disorders, Duke-NUS Medical School, 169857 Singapore, Singapore. [7]Department of Physiology, Yong Loo Lin School of Medicine, National University of Singapore, 117597 Singapore, Singapore. ✉email: fanglingguan@163.com; chenteng@xjtu.edu.cn

Received: 7 February 2022 Revised: 29 May 2022 Accepted: 7 June 2022
Published online: 22 June 2022

transcription of Notch1 target genes, such as Hes1 [17]. Notably, the Notch signalling, especially Notch1, could regulate synaptic plasticity and long-term memory in adult brain function from invertebrates to mammals [18, 19]. Interestingly, synaptic plasticity and memory are progressively affected in MIP [20, 21], implying for the possible involvement of Notch1 in the neurological deficits associated with the disease. Moreover, Notch1 imbalances have been evidenced in patients and animal models affected by psychoses, such as SCZ [22, 23], depression and anxiety [24]. However, whether and how the Notch1 pathway is involved in MIP remains unclear.

It has been proposed that damage of cortical GABAergic function leads to dysregulation and imbalance of glutamatergic and GABAergic cortical signals, resulting in MIP [2]. Previous studies identified GABA transporters and receptors expression changes in the mPFC [25], nucleus accumbens (NAc) [26] and hippocampus (Hip) [27] following METH sensitization in mice. In addition, researchers have found an association between Notch1 signalling and GABA transporters or receptors [28, 29]. Therefore, we hypothesize that Notch1 signalling is involved in MIP by regulating GABAergic genes expression. In this study, we investigated the neuron-specific changes in Notch1 expression on MIP-associated behaviours and elucidate the mechanism by which the Notch1 signalling pathway regulates MIP via the GABAergic system. Our findings provide insights into the pathogenesis of MIP and may facilitate the development of improved treatments.

MATERIALS AND METHODS

Animals

Male C57BL/6 J mice (two months old and weighing 20–25 g) were purchased from Beijing Vital River Laboratory Animal Technology Co., Ltd. (Beijing, China). Animals were housed on a light/dark cycle of 12 h/12 h in standard group cages (≤5 mice/cage) and had unrestricted access to food and water. Mice were randomly assigned to different experimental groups. All the animal protocols used in this study were approved by the Institutional Animal Care and Use Committee of Xi'an Jiaotong University and followed the guidelines established by the National Institutes of Health.

Drug treatment

For METH sensitization, METH was purchased from the National Institute for Control of Pharmaceutical and Biological Products (Beijing, China) and dissolved in 0.9% NaCl (saline). METH (1 mg/kg or 5 mg/kg, dissolved in saline) and saline were each administered via intraperitoneal (i.p.) injection. For the SCZ animal model, we used NMDA receptor antagonist MK-801 (Abcam, USA, 1 mg/kg, i.p.) once daily [30] for 21 consecutive days. For the microinjection, DAPT (Selleck, USA), a key enzyme inhibitor of Notch signal pathway, is dissolved in 90% DMSO (sigma, USA) prepared in 0.1 M sterile phosphate-buffered saline (PBS) [31] at 30 μg/μL. DAPT or vehicle was administered via bilateral intracranial microinjections at 0.5 μL/hemisphere. The $GABA_B$ receptor agonist baclofen (Sigma, USA) and the $GABA_B$ receptor antagonist phaclofen (Sigma, USA) were dissolved in saline and administered at doses of 0.06 nmol/0.2 μL/mouse [32] and 0.1 nmol /0.2 μL/ mouse [33], respectively.

Cannulation and microinjection

Briefly, the mice were anaesthetized using 1.5% isoflurane and placed in an automated stereotaxic instrument (RWD Life Science, China). A 0.8-cm-long stainless steel cannula was unilaterally implanted in the mPFC [anteroposterior (AP): +2.00 mm; mediolateral (ML): ±0.50 mm; dorsoventral (DV): −2.4 mm] [34]. After one week of recovery, DAPT or vehicle and baclofen, phaclofen or saline were infused into the mPFC 30 min before 1 mg/kg METH (or saline) was injected intraperitoneally. For the intracerebral infusions, the solutions were injected at a rate of 0.1 μL/minute. The injection cannula was left in place for an additional 5 minutes to minimise the efflux of the drug.

Adeno-associated virus generation and injection

We used AAV2/8 expressing synapsin promoter with Notch1 intracellular domain (NICD) to overexpress NICD in neurons (syn-NICD-OE), shRNA1 (GCCTCAATATTCCTTACAA) to knock down the NICD expression in neurons (syn-NICD-shRNA) and shRNA2 (TGAAAGTCTAAGCCAACTGAA) to knock down the expression of Hes1 in neurons (syn-Hes1-shRNA). The same vector backbone was used to generate a negative control. Mice were anaesthetized with 1.5% isoflurane before AAV injection. AAVs were injected bilaterally into the mPFC at the corresponding coordinates (AP: + 2.05 mm; ML: ± 0.27 mm; DV: −2.10 mm) [35]. The AAV vectors (200 nL) were infused slowly per side over 4 min into the targets using a micro-infusion pump with a 10 μL Hamilton syringe. The microsyringe was left in place for 6 min to allow the viral vectors to diffuse after microinjection. Behavioural testing was initiated four weeks after injections.

Behavioural Testing

METH-induced sensitization was performed as previously described (Fig. 1A) [25]. Briefly, METH-sensitized group received repeated doses of 1 mg/kg METH on days 1 and 7; 5 mg/kg, i.p. on days 2–6. The acute METH and saline groups were injected with saline for 7 days. Then, after a 2-week withdrawal period, the METH-sensitized and acute METH group received the same challenge dose of METH (1 mg/kg), while the saline group received one injection of saline on day 23 (Fig. 1A). Horizontal locomotor activities were recorded in metal test chambers (43 cm × 43 cm × 43 cm) and analysed for 60 min after 1 mg/kg METH injections using a smart 2.5 video tracking system. The amount of time travelled in the centre zone (21.50 cm × 21.50 cm) are interpreted as measures of anxiety-like behaviour [36].

The specific methods of other behavioural testing, such as open filed test, novel object recognition (NOR), Y maze test, social interaction test (SIT), elevated plus maze (EPM), tail suspension test (TST) and forced swimming test (FST), were seen in the supplemental methods.

Immunofluorescence (IF) analysis

The mice were anesthetized 1 hour after the last METH/saline injection. The brains were post-fixed in the perfusion solution for 4 h at 4 °C followed by 24 hours of incubation in 30% sucrose solution. The Tissue-Tek O.C.T. compound (Sakura, Japan) was used to embed brain tissue, which was consequently cut in 20-μm slices using a cryostat (Leica, Germany). Brain sections were blocked with 5% bovine serum albumin containing 0.3% Triton X-100 at 37 °C for 60 min and incubated with primary antibodies to rabbit anti-Notch1 (1:200, Proteintech, 20687-1-AP); mixed rabbit anti-Notch1 and mouse anti-$GABA_{B1}$ (1:100, Abcam, ab55051) overnight at 4 °C. Subsequently, brain tissue sections for Notch1 receptor were incubated with goat anti-rabbit coralite 488 conjugate (1:500, Proteintech, SA00013-2); brain tissue sections for Notch1 and $GABA_{B1}$ receptor double staining were incubated with goat anti-rabbit coralite 594 conjugate (1:500; SA00013-4; Proteintech) and goat anti-mouse coralite 488 conjugate (1:500; SA00013-1; Proteintech) for 1 h at room temperature. Nuclei in immunolabeled specimens were visualized with DAPI. The sections were observed under a fluorescence microscope (Carl Zeiss, Axio scope A1, Germany). At least 10 regions from three mice of each group were chosen randomly and analysed by observers who were unaware of the experimental cohort.

Quantitative real-time reverse transcription PCR (RT-qPCR)

Mice were sacrificed 1 h after the last METH/saline injection, and the brains were rapidly removed. The mPFC, NAc and Hip were dissected out based on mouse brain structure and landmarks under dissecting microscopy. Total RNA was isolated using a DNA/RNA/protein kit (Omega, USA). Total RNA was reversed transcribed into 10 μL of complementary DNA (cDNA) with PrimeScript™ RT Master Mix (Takara Biomedical Technology, China) at 37 °C for 15 min, 85 °C for 5 s, and 4 °C for 5 min. RT-qPCR for mRNA detection was performed with the SYBR Premix Ex Taq II (Takara Biomedical Technology, China) using Bio-Rad iQ5 detection instrument (Bio-Rad, USA) under the following conditions: 95 °C for 30 s, 40 cycles of 95 °C for 15 s, 60 °C for 30 s and 72 °C for 30 s. Gene expression was analysed as previously described [37]. The sequences of the primer pairs were shown in Supplemental Table 1.

Western blot

Total mPFC tissue was collected 1 hour after the last injection, and the protein concentration in each sample was determined using a BCA protein assay kit (Pierce, Rockland, IL, USA). These protein samples were separated using 10% SDS–PAGE and transferred to nitrocellulose membranes (Millipore, USA). Then, the membranes were blocked for 3 h in 5% (w/v) milk at room temperature and incubated overnight at 4 °C with the following primary antibodies: rabbit anti-Notch1 (1:1000, Abcam, ab8925),

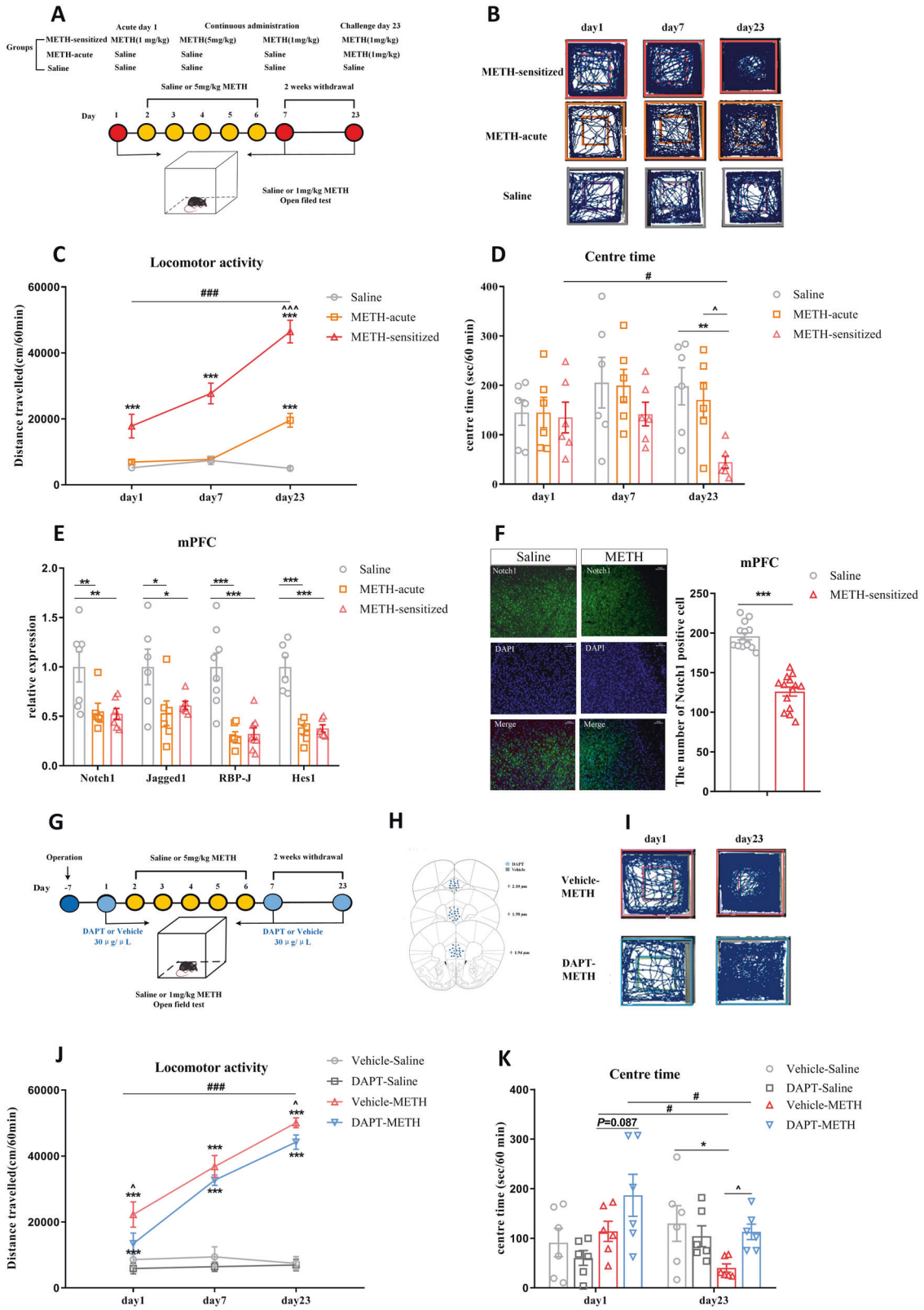

rabbit anti-Hes1 (1:1000, Abcam, ab71559), and mouse anti-$GABA_{B1}$ receptor (1:2000, Abcam, ab55051). Membranes were then washed with TBST and probed with the appropriate horseradish peroxidase-conjugated secondary antibodies (1:2000) for 1.5 h at room temperature. Proteins were detected with an enhanced chemiluminescence assay kit (ECL Plus, Millipore Corporation, USA). Signals were visualized using ImageLab 1.46 (BioRad, USA).

Chromatin immunoprecipitation (ChIP)-qPCR

ChIP assays were performed using a ChIP assay kit (Millipore EZ-CHIP 17-371, USA) according to the manufacturer's instructions [38]. Briefly, crosslinking was performed with 1% formalin, the mPFC was lysed in SDS buffer, and sonication was used to fragment the DNA to an average length of 200 to 500 base pairs. The input group accounted for 1% of the total DNA, while IgG and Hes1 (1:10, Cell Signaling Technology, #11988,

Fig. 1 The involvement of the Notch1 signalling pathway in the mPFC of METH-induced sensitized mice. A–E Changes in Notch1 signalling in the mPFC of METH-sensitized mice. **A** Procedure for generating the METH-induced locomotor sensitization model. **B** Representative mouse tracks from days 1, 7 and 23 were illustrated. **C** METH-induced locomotor sensitization in mice. One-way repeated-measures ANOVA revealed a significant main effect of METH [$F_{(2, 21)} = 47.41$, $P < 0.001$]. Subsequent post hoc LSD comparisons found significantly greater locomotor activity in the METH-sensitized group than in the saline group on day 1, day 7 and day 23. The METH-sensitized group showed a significant increase in locomotor activity compared with the METH-acute group on day 23 and itself on day 1. **D** The amount of time mice spent in the centre zone significantly decreased in the METH-sensitized group compared with the saline and acute METH group on day 23 [One-way repeated-measures ANOVA, $F_{(2, 15)} = 3.66$, $P < 0.05$]. **E** Changes in the expression of Notch1 signalling pathway components following METH sensitization in the mPFC. There was significant downregulation of Notch1 [$F_{(2, 17)} = 6.41$, $P < 0.01$], Jagged1 [$F_{(2, 15)} = 3.81$, $P < 0.05$], RBP-J [$F_{(2, 20)} = 18.05$, $P < 0.001$], and Hes1 [$F_{(2, 15)} = 29.68$, $P < 0.001$] in both the METH-acute and METH-sensitized groups by one-way ANOVA**. F** Representative images of immunofluorescence staining for Notch1 receptors in mPFC between the METH-sensitized group and the saline group. Quantitative analysis of Notch1-positive cells in the METH-sensitized group showed a significant decrease ($t_{26} = 9.76$, $^{***}P < 0.001$) by student's-*t* test (scale bar = 50 μm, $n = 3$ / group, 10–15 photos). **G–K** Intra-mPFC DAPT treatment attenuated METH-induced locomotor sensitization. **G** Procedure for the administration of DAPT in the mPFC in METH-induced sensitization mice. **H** Location of the DAPT and vehicle microinjection cannula tips in the mPFC. **I** Representative tracks of vehicle-METH and DAPT-METH mice on day 1 and day 23. **J** Intra-mPFC infusion of DAPT significantly attenuated the hyperlocomotion evoked by METH on day 1 and day 23. Mixed-design ANOVA with a LSD post hoc multiple comparison revealed significant main effects of DAPT [$F_{(1, 21)} = 5.38$, $P < 0.05$]; METH [$F_{(1, 21)} = 206.21$, $P < 0.001$]; but not DAPT×METH [$F_{(1, 21)} = 1.36$, $P > 0.05$]. **K** The time mice spent in the centre zone was higher in the DAPT-METH group than in the vehicle-METH group on day 23. Mixed-design ANOVA with LSD post hoc multiple comparisons show the main effect of DAPT [$F_{(1, 20)} = 1.24$, $P > 0.05$]; METH [$F_{(1, 20)} = 0.74$, $P > 0.05$] and DAPT × METH [$F_{(1, 20)} = 6.45$, $P < 0.05$]. $^{*}P < 0.05$, $^{**}P < 0.01$, $^{***}P < 0.001$ vs. paired saline group; $^{\wedge}P < 0.05$ vs. paired METH group; $^{\#}P < 0.05$, $^{\#\#\#}P < 0.001$ vs. same group on day 1. Data were presented as mean ± S.E.M, $n = 6$–8.

USA) antibodies were added as negative controls and samples. After purification, RT–qPCR was performed to detect the protein binding sites of the DNA samples. The ChIP signal was calculated as follows: % input = 1% × 2^($CT_{input} - CT_{sample}$). The sequences of the RT-PCR primers used for $GABA_{B1}$ receptor promoter were shown in Supplemental Table 1.

Fiber photometry

Mice were unilaterally injected with 0.3 μL of AAV-syn-GCaMP7f and 0.2 μL of AAV-syn-NICD-shRNA-mCherry or control into the ipsilateral mPFC. A unilateral optical fiber (200 μm core, 0.39 numerical aperture (NA), RWD, China) was implanted at these coordinates and secured in place using dental cement after two weeks of recovery from AAV-micro-injection. Then, the mice recovered in their home cage for seven days before beginning behavioural testing. A fiber photometry system (R810, RWD Life Science, China) was used to record the fluorescence signal (GCaMP7f), which was produced by an exciting laser beam from 470 nm LED light and 410 nm LED light [39]. On the experimental day, mice were allowed to acclimate in the behavioural testing chamber for 30 min. After the acclimation period, baseline fluorescence was recorded for 5 minutes. Then, the mice were injected with METH (1 mg/kg, i.p.) or saline. Fluorescence was then recorded with the optical fiber for 15 min after the administration of METH. ΔF/F was calculated according to (470 nm signal-fitted 410 nm signal)/ (fitted 410 nm signal). The standard Z score calculation method was performed in MATLAB 2014. The formula was as follows: Z score = (x-mean)/std, x = ΔF/F.

Statistical analysis

The minimal sample size was pre-determined by the nature of experiments. No statistical methods were used to pre-determine sample sizes, but our sample sizes are similar to those reported in previous publications [25, 37, 39]. Details of the number of independent experiments are provided in the figure legends. For all experiments in this study, the animals were randomly assigned to experimental groups and control groups. Investigators involved in conducting experiments, collecting data and performing analyses were blinded to the mice groups.

Datasets were checked for normality, variations, and statistical tests using SPSS (version 18.0). One-way or mixed-designed repeated ANOVA with multiple comparisons followed by LSD post hoc were applied to the METH-induced locomotor sensitization data. Other data from behavioural tests, RT–qPCR and Western blot were analysed by one-way or two-way ANOVA followed by LSD post hoc test. The averaged Z scores of fiber photometry were compared by a paired-sample *t* test. IF and ChIP-qPCR data were analysed by student's *t* test. All data were expressed as the mean ± standard error of the mean (SEM), and $P < 0.05$ was considered statistically significant.

RESULTS

The Notch1 signalling pathway was downregulated in the mPFC of METH sensitized mice

Here, mice were treated with METH in a standard protocol to examine METH-induced locomotor sensitization (Fig. 1A) [25]. Repeated intermittent METH administration led to a progressive augmentation of behavioural changes compared with the saline group, and mice showed a significant sensitization response compared with the acute METH group on day 23 (Fig. 1B, C). Meanwhile, the time that mice spent in the centre area of the open field was significantly decreased following METH challenge (Fig. 1D), which indicated that METH challenge induced increased anxiety-like behaviour in mice.

We next examined the mRNA levels of Notch1 signalling in the mPFC, NAc, and Hip, which are psychosis-related brain regions. Our results showed that both acute METH treatment and METH sensitization induced obvious downregulation of mRNA levels of Notch1, Jagged1, RBP-J and Hes1 in the mPFC (Fig. 1E). However, there were no significant changes of Notch1 signalling in mPFC between acute METH exposure and challenge METH exposure. As for other brain nuclei NAc or Hip, not all of the mRNA level of Notch1 signalling of METH sensitized mice showed significant changes from the control saline group (Fig. S1A, B). The immunofluorescence further indicated that the protein level of Notch1 receptor was significantly decreased in the mPFC of the sensitized mice compared with the saline mice (Fig. 1F), but not in the NAc or Hip (Fig. S1C, D). Therefore, we chose the mPFC as the target region to further examine the role of the Notch1 pathway in MIP.

METH-induced sensitization has similar neurobiological changes with MIP, which is closely related to SCZ. Therefore, we established the SCZ animal model induced by 21-day consecutive treatment of MK-801 (Fig. S2A) [30] to detect neurobiological similarities between MIP and SCZ. The open filed test also showed the hyperlocomotion and decreased centre time, which is the same with METH sensitization (Fig. S2B). Positive symptoms of SCZ were also shown in the EPM, which was reflected by MK-801 treatment mice spending less time in open arms and less number of open arm entries (Fig. S2C). Besides, the NOR test showed a lower recognition index in the MK-801 group of mice than the control group, indicating the cognitive impairment of SCZ (Fig. S2D). The decreased social interaction in SIT (Fig. S2E) and the increased immobility time in TST (Fig. S2F) of MK-801 treated mice showed the negative symptoms of SCZ. After successful establishment of the SCZ animal model, we measured the changes in expression of Notch1 signalling in the mPFC of mice. Surprisingly, there was no significant difference of mRNA level of Notch1 signalling in the mPFC after MK-801 treatment (Fig. S2G). Similarly, the data from PsychENCODE Consortium in the NIMH Repository (http://psychencode.org), which collected the transcription profiles of prefrontal cortex tissue from postmortem SCZ patients [40],

showed no difference in Notch1 signalling between SCZ patients and healthy controls (Fig. S2H). These results suggested specific alterations in Notch1 signalling at the mPFC in the METH-sensitized mice.

Differential expression of Notch1 signalling in mPFC was capable of regulating MIP-related behaviours

Inhibition of Notch1 signalling in the mPFC attenuated METH-induced locomotor sensitization. To test whether inhibition of Notch1 signalling in mPFC could affect METH-induced locomotor sensitization, we first administered the Notch signalling inhibitor DAPT in mPFC [31]. Vehicle or DAPT (30 μg/μL) was administered to the mPFC 30 min before saline or 1 mg/kg METH treatment (Fig. 1G, H). DAPT itself did not induce any locomotion responses in mice (Fig. 1J). However, DAPT suppressed METH-induced hyperlocomotion on acute and challenge days (Fig. 1I, J) and enhanced the time spent in the centre area in response to METH on challenge day (Fig. 1K).

Inhibition of Notch1 signalling in the mPFC neurons attenuated METH-induced locomotor sensitization. We further used syn-NICD-shRNA to inhibit the neuronal expression of Notch1 intracellular domain (NICD) in the mPFC (Fig. 2A). The RT-qPCR and western blot were used to verify the efficiency of NICD downregulation after syn-NICD-shRNA microinjection. The shRNA first inhibited the transcription level of NICD, indicating significant decreases in the syn-NICD-shRNA group compared with the control group (Fig. 2B). The western blot further identified that syn-NICD-shRNA could induce the downregulation of NICD protein level in the mPFC (Fig. 2B). After verifying the syn-NICD-shRNA function, both groups were then subjected to repeated intermittent METH treatment, and the locomotor activity of the mice was tested (Fig. 2C, D). Downregulation of NICD in the mPFC significantly reduced the total distance travelled in response to METH on the acute and challenge day (Fig. 2C, D) and increased the time spent in the centre area (Fig. 2E). These results is the same with DAPT treatment in the METH-induced locomotor sensitization.

Overexpression of Notch1 signalling in the mPFC enhanced METH-induced locomotor sensitization. We further tested whether overexpressing NICD (syn-NICD-OE) in mPFC neurons could enhance METH-induced locomotor sensitization. We first showed the efficiency of NICD overexpression after syn-NICD-OE micro-injection. In the syn-NICD-OE group, the mRNA level of NICD was significantly increased (Fig. 2F). Furthermore, the protein level was also considerably higher in the mPFC of syn-NICD-OE mice than in those of control-flag mice (Fig. 2F).Then both groups were subjected to repeated intermittent METH treatment (Fig. 2A). As expected, the overexpression of NICD in the mPFC dramatically enhanced the locomotor distance on acute and challenge day (Fig. 2G–H) and decreased the time spent in the centre area compared to the control METH group (Fig. 2I).

Regulation of Notch1 signalling expression in the mPFC influenced other MIP-related behaviours. Besides locomotor sensitization, MIP also exhibited other behaviours relevant to psychiatric symptoms, such as cognitive impairment, decreased social interaction, depression and anxiety [41]. Thus, we examined the influences of Notch1 signalling on these behaviours of mice after METH treatment (Fig. S3A). Downregulating NICD in mPFC neurons attenuated the MIP-related cognitive impairment of mice in both NOR (Fig. S3C) and Y maze test (Fig. S3D). The MIP mice showed significantly decreased social interaction, which was blocked by downregulating NICD in the mPFC neurons (Fig. S4A). Moreover, syn-NICD-shRNA group of mice also reversed the MIP-related anxiety-like behaviours in the EPM (Fig. S4B-C) and depression-like behaviours in the TST (Fig. S4D) and FST (Fig. S4E) respectively. In contrast, syn-NICD-OE aggravated MIP-related behaviours in the NOR (Fig. S3F), Y maze (Fig. S3G), SIT (Fig. S4F), EPM (Fig. S4G-H), TST and FST (Fig. S4I–J). All these data corroborate the idea that differential expression of Notch1 signalling in the mPFC was capable of regulating MIP.

Downregulation of Notch1 signalling in the mPFC attenuated neuronal activity in METH-induced locomotor sensitization

The dysregulation of mPFC neuronal activity is a key factor causing MIP [42]. Therefore, we characterised whether mPFC neuronal activity was modulated by regulating Notch1 signalling in METH-induced locomotor sensitization (Fig. 3A). We co-injected the AAV-syn-GCaMP7f and syn-NICD-shRNA-mCherry into the mPFC region of mice, nearly 95% of the GCaMP7-positive cells also expressed mCherry (Fig. 3B). We further employed fiber photometry to monitor the Ca^{2+} signals of mPFC neurons in the METH treated group and saline group on acute phase and challenge day. Syn-NICD-shRNA induced a significant reduction of mPFC neurons activity in response to acute METH exposure (Figs. 3C, E, G). On the challenge day, the fluorescent signal was first reduced within approximately five minutes and then increased gradually (Figs. 3D, F). However, neuronal activity tested in the syn-NICD-shRNA mice showed no increasing trend after METH injection on day 23 (Figs. 3D, F) and demonstrated a significant reduction compared to what was before METH treatment (Fig. 3H). Besides, both the control and syn-NICD-shRNA groups of mice did not show significant changes in the fluorescent signal after saline injection on acute (Fig. S5B, S5D, S5F) and challenge days (Fig. S5C, S5E, S5G). This result indicated the mPFC neuron activity was not affected by the syn-NICD-shRNA itself. All these data identified that the downregulation of NICD in the mPFC could directly attenuate neuronal activity in sensitized mice, which may ultimately lead to the attention of METH-induced behaviour sensitization.

The Notch1 signalling pathway in the mPFC negatively regulated $GABA_{B1}$ receptor expression

Previously, differential expression of GABA transporters (GAT1 and GAT3), ionotropic $GABA_A$ receptor subunits (α3 and β1), and metabotropic $GABA_B$ receptors were found in the mPFC of the same animal model of METH-induced locomotor sensitization [43]. Moreover, Notch1 signalling was associated with GABA receptors and transporters expression [28, 29, 44]. We speculated that the GABAergic system may underlie the mechanism through which Notch1 signalling regulated METH sensitization. Indeed, we found that the mRNA expression levels of GABA receptors and transporters in the mPFC decreased in both the acute METH and METH-sensitized groups (Fig. 4A). Moveover, the mRNA levels of $GABA_{A\beta1}$, $GABA_{B1}$ and GAT1 were significantly upregulated in the METH-sensitized group compared to the acute METH group (Fig. 4A).

We then assessed whether the changes in the expression of GABA receptors and transporters were regulated by Notch1 signalling in the mPFC. We found that syn-NICD-shRNA in the mPFC significantly reversed the reduction mRNA levels in $GABA_{A\beta1}$, $GABA_{A\alpha3}$ and $GABA_{B1}$ in response to METH (Fig. 4B, Fig. S6A–E), while syn-NICD-OE only significantly decreased $GABA_{B1}$ expression (Fig. 4C, Fig. S6F–J). In addition, the direct injection of DAPT into the mPFC showed the same effects as syn-NICD-shRNA on GABAergic genes (Fig. 4D, Fig. S6K–O). Western blotting confirmed the changes in the expression of the $GABA_{B1}$ receptor when NICD expression in the mPFC as manipulated (Fig. 4E, F). As expected, syn-NICD-OE reduced the protein expression level of the $GABA_{B1}$ receptor in the mPFC (Fig. 4E), whereas syn-NICD-shRNA group showed the increased protein level of $GABA_{B1}$ receptor compared with the control group (Fig. 4F). To further confirmed the association between

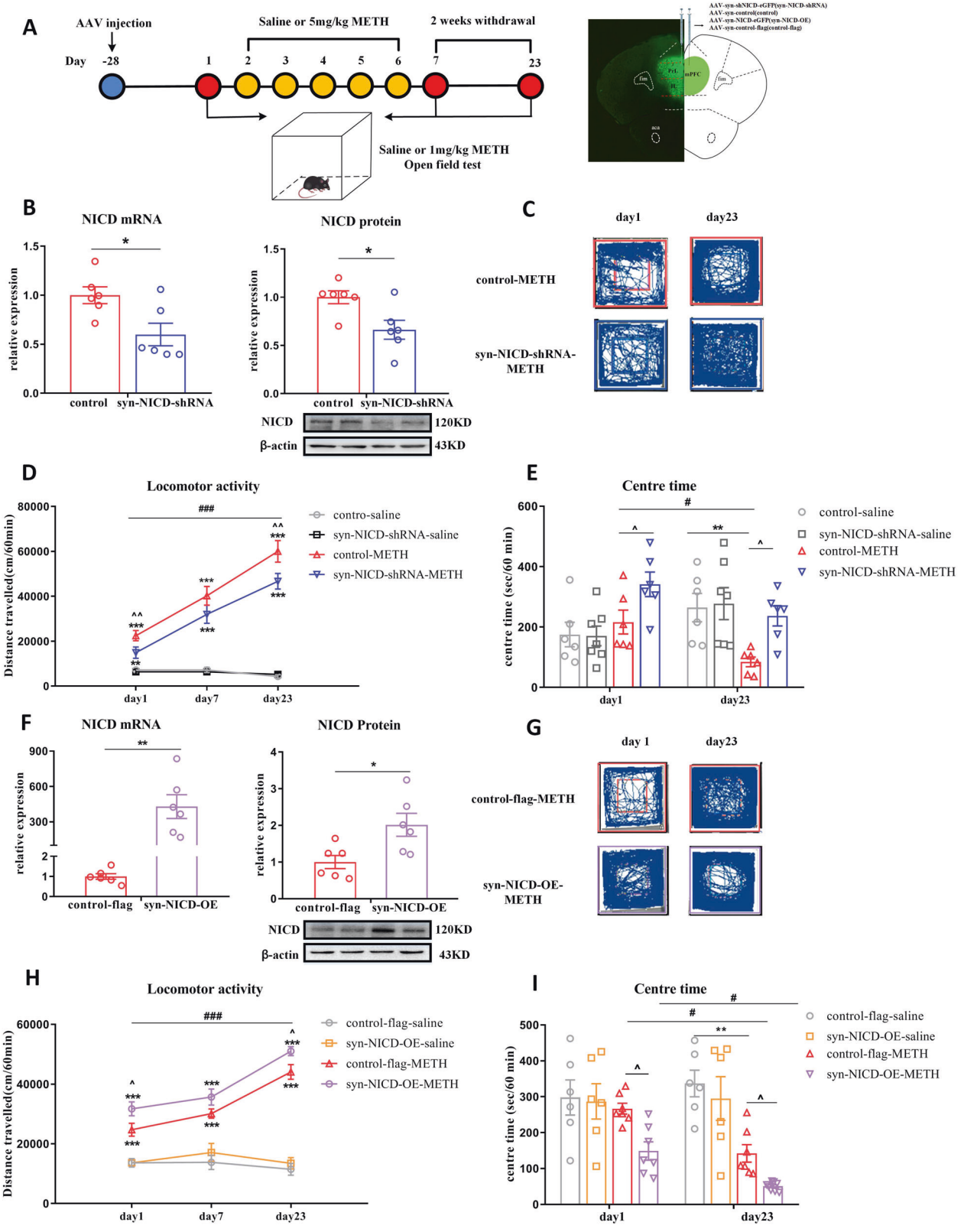

Notch1 signalling and $GABA_{B1}$ receptor in the mPFC of mice, we used double-label immunofluorescence staining for Notch1 and $GABA_{B1}$ receptor in the mPFC of mice. As shown in Fig. 4G, $GABA_{B1}$ receptor (green) and Notch1 receptor (red) were co-expressed in the mPFC of naive mice. These results further strengthened the evidence linking Notch1 signalling with $GABA_{B1}$ receptor in the mPFC of mice. Taken together, the evidence suggested that the regulation of Notch1 signalling in the mPFC may negatively regulated the expression of the $GABA_{B1}$ receptor.

Fig. 2 Manipulating Notch1 expression affects METH-induced locomotor sensitization. A Timeline of AAV injection, behavioural tests and location of AAV expression. **B**–**E** Inhibition of NICD in the mPFC suppressed METH-induced locomotor activity. **B** NICD mRNA ($t_{10} = 2.79$, $^{*}P < 0.05$) and protein ($t_{10} = 2.84$, $^{*}P < 0.05$) levels were significantly lower in syn-NICD-shRNA group as indicated by student's *t* test. **C**, **G** Representative paths of mice in the syn-NICD-shRNA-METH and control-METH or syn-NICD-OE-METH and control-flag-METH groups on day 1 and day 23. **D** Downregulation of NICD in mPFC neurons significantly decreased locomotion on day 1 and day 23. Mixed-design ANOVA with a LSD post hoc multiple comparison revealed significant main effects of AAV [$F_{(1, 20)} = 8.95$, $P < 0.01$]; METH [$F_{(1, 20)} = 323.81$, $P < 0.001$]; and AAV×METH [$F_{(1, 20)} = 8.10$, $P < 0.05$]. **E** Time spent in the centre zone was significantly higher in the syn-NICD-shRNA-METH group than in the control-METH group on day 1 and day 23 [Mixed-design ANOVA, main effect of AAV, $F_{(1, 21)} = 7.61$, $P < 0.05$; METH, $F_{(1, 21)} = 0.01$, $P > 0.05$; AAV × METH, $F_{(1, 21)} = 7.18$, $P < 0.05$]. **F**–**I** Overexpression of Notch1 in the mPFC enhanced METH-induced locomotor activity. **F** NICD mRNA ($t_{10} = -4.25$, $^{**}P < 0.01$) and protein ($t_{10} = -2.81$, $^{*}P < 0.05$) levels were significantly higher in the m*P*FC of the syn-NICD-OE group than the control-flag group as determined by student's *t* test. **H** Overexpression of NICD significantly increased locomotion on day 1 and day 23 compared with the control-flag-METH group. Mixed-design ANOVA with a LSD post hoc multiple comparison revealed significant main effects of AAV [$F_{(1, 20)} = 8.28$, $P < 0.01$]; METH [$F_{(1, 20)} = 241.37$, $P < 0.001$]; but not the AAV×METH [$F_{(1, 20)} = 2.70$, $P > 0.05$]. **I** The time that mice spent in the centre zone was significantly downregulated in the syn-NICD-OE-METH group compared with the control-flag-METH group on day 1 and day 23 [Mixed-design ANOVA, main effect of AAV, $F_{(1, 22)} = 6.50$, $P < 0.05$; METH, $F_{(1, 22)} = 32.14$, $P < 0.001$; AAV × METH, $F_{(1, 22)} = 2.09$, $P > 0.05$]. $^{*}P < 0.05$, $^{**}P < 0.01$, $^{***}P < 0.001$ vs. paired saline group; $^{\wedge}P < 0.05$ vs. paired METH group; $^{\#}P < 0.05$, $^{\#\#\#}P < 0.001$ vs. same group on day 1. Data were presented as mean ± S.E.M, $n = 6$–8.

Notch1 signalling regulated the expression of the $GABA_{B1}$ receptor directly via Hes1

Hes1, a downstream transcriptional repressor of Notch1 signalling, expressed in neurons and controls GABAergic differentiation [45]. Therefore, we surmised that the transcriptional repressor Hes1 might be the key factor negatively regulating $GABA_{B1}$ receptor expression. To test this hypothesis, we measured the mRNA and protein levels of Hes1 in the mPFC. Remarkably, Hes1 was upregulated in the syn-NICD-OE group, in which the abundance of $GABA_{B1}$ receptor was decreased (Figs. 5A, C). In contrast, Hes1 was reduced in the syn-NICD-shRNA group with higher level of $GABA_{B1}$ receptor (Figs. 5B, D). Furthermore, shRNA was used to suppress Hes1 expression in the mPFC (Fig. 5E, F) and $GABA_{B1}$ receptor expression was significantly increased in the syn-Hes1-shRNA group (Fig. 5E, F).

The JASPAR database predicted 3 potential binding sites for Hes1 on the $GABA_{B1}$ promoter (Fig. 5G). We performed ChIP-qPCR to determine whether Hes1 directly bind to $GABA_{B1}$ receptor promoter to regulate expression. According to the ChIP-qPCR results, there was significant enrichment of Hes1 at the specific binding sites (primer 3) of the $GABA_{B1}$ receptor promoter (Fig. 5H). Taken together, these results suggest that Hes1 transcriptionally inhibited the expression of the $GABA_{B1}$ receptor by binding to its promoter region.

Notch1 signalling regulated METH-induced locomotor sensitization through $GABA_{B1}$ receptor

To further test whether Notch1 signalling regulated METH-induced locomotor sensitization through the $GABA_{B1}$ receptor, we co-regulated Notch1 and $GABA_B$ receptor activity in the mPFC of mice and examined the behaviours of METH sensitization (Fig. 6A). The treatment of phaclofen, a $GABA_B$ receptor antagonist, abolished the suppression of METH sensitization induced by syn-NICD-shRNA (Fig. 6B). Moreover, a $GABA_B$ receptor agonist baclofen completely normalized the enhancement of METH sensitization by syn-NICD-OE (Fig. 6D). Meanwhile, the effect of NICD expression changes on the time that mice spent in the centre area of the open field was also reversed by phaclofen and baclofen (Figs. 6C, E). Given of no expression changes of the $GABA_{B2}$ receptor in syn-NICD-shRNA or syn-NICD-OE group (Fig. S6C, S6H), Notch1 signalling may regulate METH-induced locomotor sensitization through $GABA_{B1}$ receptor.

DISCUSSION

A mechanistic understanding of how MIP occurs and develops in terms of neuronal molecular events is currently lacking. Our approach to addressing this process is a unique intersection of the study of MIP, Notch1 signalling and GABA receptors. We found that regulating the mRNA and protein levels of Notch1 in the mPFC could affect MIP-related behaviours, such as METH-induced sensitization, NOR, Y maze, EPM, FST, and TST. Our study further reveals that the Notch1 signalling partway can regulate METH-induced locomotor sensitization by influencing the $GABA_{B1}$ receptor expression via Hes1-dependent Notch1 signalling mechanisms. To the best of our knowledge, these data provide the first evidence for a potential link between dysregulation of Notch1 signalling in the mPFC and the pathogenesis of MIP.

Some previous studies have reported that the indistinguishable symptoms of MIP and SCZ might share similar risk factors and molecular mechanisms [3, 13], which could be represented by METH-induced locomotor sensitization mice model. However, we only observed significant decreases in the mRNA levels of Notch1 signalling components in the mPFC of METH-acute and METH-sensitized groups. In contrast, neither animal models of SCZ nor postmortem data from SCZ patients have shown significant changes in Notch1 signalling in the mPFC. These results suggest that MIP may have a specific mechanism that is different from that of SCZ. Besides, synaptic dysfunctions in MK-801 treated and METH-sensitized mice are distinct; in the MK-801-treated animal model of SCZ, hyperactivity is caused by NMDAR hypofunction, whereas METH sensitization is mainly caused by the overflow of dopamine in synapses [46]. Previous studies have demonstrated that the hypofunction of NMDAR induced by MK-801 mainly elevated the release of glutamate and 5-HT in the mPFC, which could cause hyperactivity and other SCZ-associated behaviours [47]. However, both acute METH-treated mice and METH-sensitized mice mainly induce the upregulation of extracellular dopamine levels in the mPFC [48, 49]. The activity of dopamine neurons projecting to mPFC could cause hyperactive and METH-induced locomotor sensitization [50]. Therefore, the downregulated Notch1 signalling in METH-acute and METH-sensitized groups may be closely related to excessive dopaminergic activity but not glutamate or 5-HT. Moreover, ropinirole, a D2 type dopamine receptor (D2R) agonist, can induce the hyperfunction of dopamine system and further affect the Notch1 mRNA expression [51]. Hence, we could assume that dysfunction of the dopamine system modulates Notch1 signalling. However, other studies also reported that Notch1 signalling could directly regulate the dopamine system. Conditional deletion of Notch1 signalling RBP-J specifically in neuronal cells drastically reduced dopamine release in the striatum in the acute METH exposure [52]. The lasting transcriptional changes induced by alcohol in Drosophila showed that the Notch signalling pathway could directly regulate the D2R expression [53]. As a result, dopamine and Notch1 signalling pathway are independent but mutually

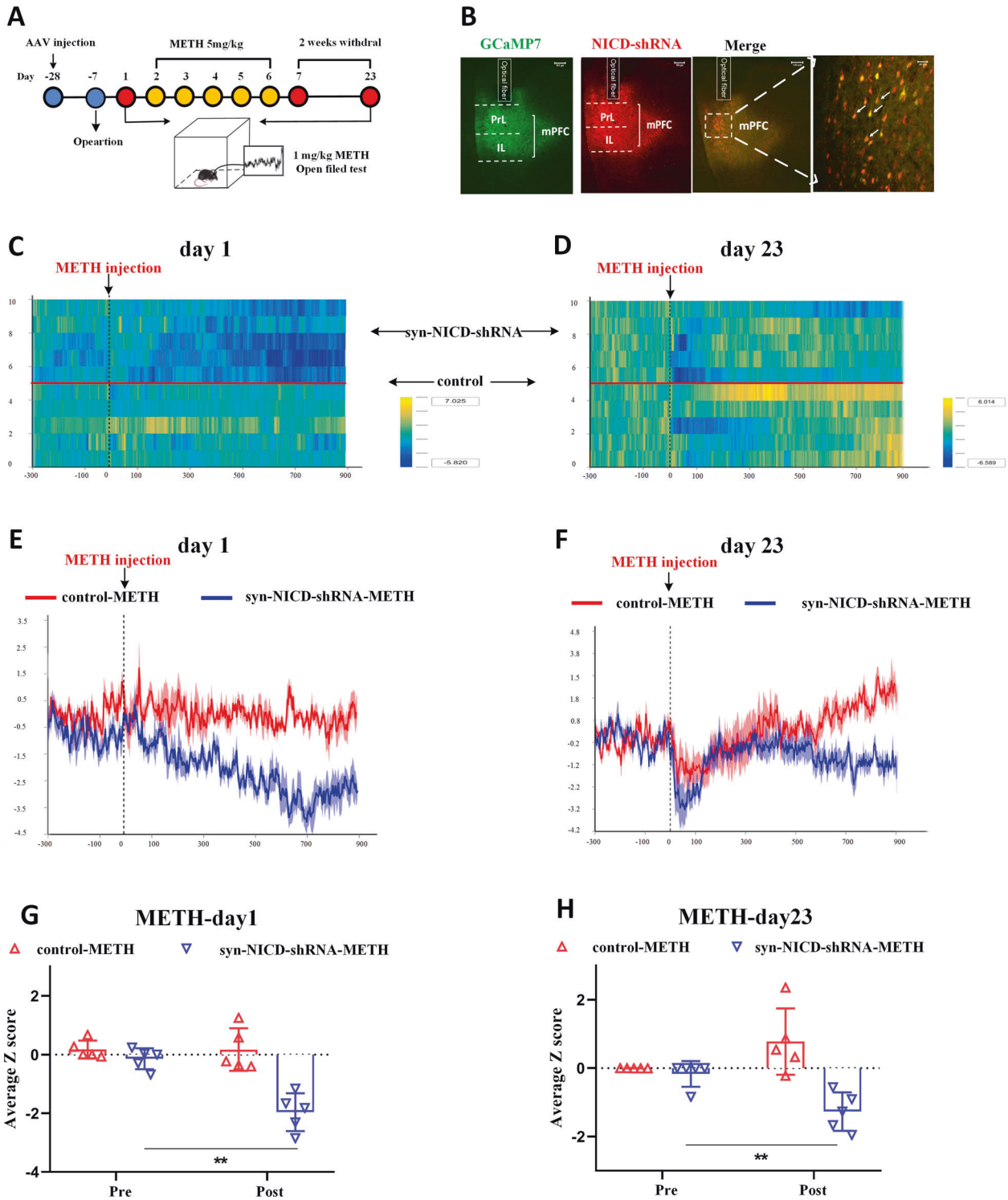

Fig. 3 Inhibition of the Notch1 signalling attenuates mPFC neuronal activity of METH-induced sensitized mice. A Experimental design for recording GCaMP activity from mPFC neurons which reduced the Notch1 signalling during METH sensitization. Calcium-dependent (470 nm) and calcium-independent (410 nm) fluorescence signals were recorded before and after administration of METH (1 mg/kg) in the open field. **B** Fluorescence images in the mPFC from mice that received unilateral infusion of syn-GCaMP7f (green) and syn-NICD-shRNA (red) virus, scale bar = 100 μm. Arrows indicate neurons both expressed GCaMP7f and NICD-shRNA signals, scale bar = 40 μm. **C**, **D** Heatmap illustration of Ca^{2+} signals aligned to the initiation of trials on day 1 and day 23. Each row plots one trial, and a total of 10 trials were illustrated. The colour scale on the right indicates Z scores. **E**, **F** Average traces of calcium signals from control mPFC neurons (red line) and inhibitory NICD mPFC neurons (blue line) were recorded before (5 min) and after METH treatment (15 min) on days 1 and 23. **G**, **H** The average Z scores from (**E**) and (**F**) in the open field before (pre) and after (post) METH injection on day 1 and day 23. The fiber photometry signal of mPFC neurons in the syn-NICD-shRNA-METH group was significantly reduced compared with the baseline signal on day 1 and day 23, according to a paired-sample *t* test ($t_{day1} = 7.953$, $t_{day23} = 4.58$, $^{**}P < 0.01$ vs. before METH injection). Traces represent mean ± SEM (**E**, **F**). Error bars represent mean ± SEM (**G**, **H**), $n = 5$.

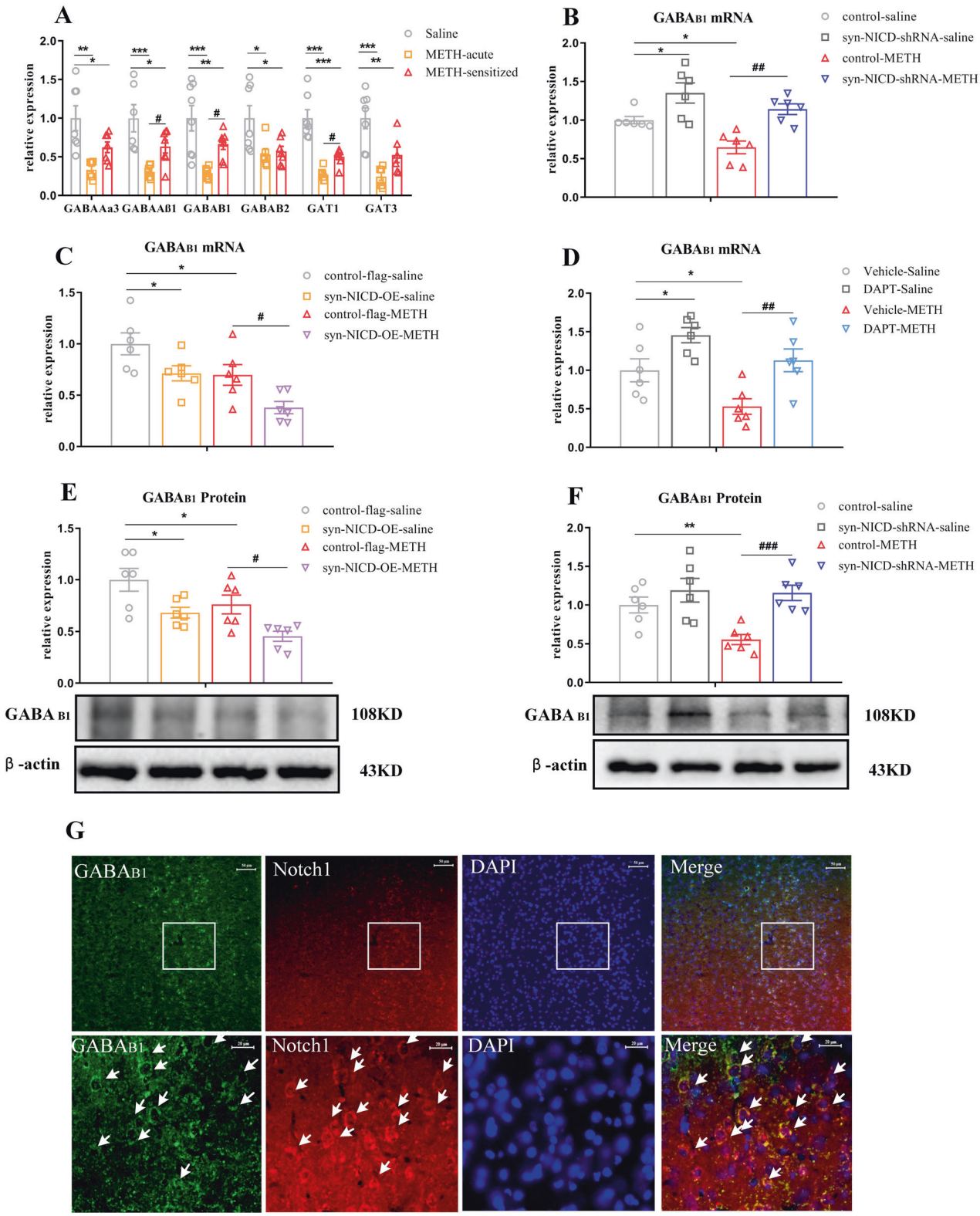

influence each other. There is a cross-talk between these two pathways. Potential interactions between the Notch1 signalling pathway and dopamine system in the pathogenesis of MIP warrant further research.

Although the mRNA and protein levels of the Notch1 receptor were both significantly decreased in the METH-sensitized group, there was no difference between the METH-acute group and the METH-sensitized group. These results suggested that the Notch1 signalling may only play a role in acute effects, but not sensitization. Nevertheless, regulating the Notch1 signalling expression by DAPT and AAV not only affected the locomotor activity in the acute phase but also in the expression phase during

Fig. 4 The Notch1 signalling pathway negatively regulated the $GABA_{B1}$ receptor expression of METH-induced sensitized mice. A GABA receptors and transporters expression changes following METH sensitization in the mPFC. One-way ANOVA showed the significant downregulation effects of METH on $GABA_{A\alpha3}$ [$F_{(2, 17)} = 9.17$, $P < 0.05$], $GABA_{A\beta1}$ [$F_{(2, 17)} = 10.38$, $P < 0.05$], $GABA_{B1}$ [$F_{(2, 18)} = 11.66$, $P < 0.05$], $GABA_{B2}$ [$F_{(2, 17)} = 5.36$, $P < 0.05$], GAT1 [$F_{(2, 17)} = 25.79$, $P < 0.05$] and GAT3 [$F_{(2, 16)} = 13.48$, $P < 0.05$]. Subsequent post hoc LSD comparisons found higher expression changes of $GABA_{A\beta1}$, $GABA_{B1}$ and GAT1 between the METH-sensitized group and acute METH group. *$P < 0.05$, **$P < 0.01$. ***$P < 0.001$ vs. saline group. #$P < 0.05$ METH-sensitized group vs. acute METH group. 4B-4F. $GABA_{B1}$ receptor expression changes following regulation of the Notch1 signalling pathway in the mPFC of MIP mice. **B**, **F** Two-way ANOVA followed by LSD test showed significant upregulation of the $GABA_{B1}$ receptor in the syn-NICD-shRNA group at both the mRNA and protein levels in the mPFC of MIP mice [**B** main effect of AAV, $F_{(1, 20)} = 23.29$, $P < 0.001$; METH, $F_{(1, 20)} = 10.27$, $P < 0.01$; AAV × METH, $P > 0.05$] and protein level [**F** Main effect of AAV, $F_{(1, 20)} = 13.09$, $P < 0.01$; METH, $F_{(1, 20)} = 4.78$, $P < 0.05$; AAV×METH, $P > 0.05$]. **C**, **E** Two-way ANOVA followed by LSD test showed significant downregulation of the $GABA_{B1}$ receptor at both the mRNA [**C** main effect of AAV, $F_{(1, 20)} = 12.03$, $P < 0.01$; METH, $F_{(1, 20)} = 13.28$, $P < 0.01$; AAV × METH, $P > 0.05$] and protein [**E** main effect of AAV, $F_{(1, 20)} = 15.31$, $P < 0.01$; METH, $F_{(1, 20)} = 8.44$, $P < 0.01$; AAV × METH, $P > 0.05$] levels in the mPFC of MIP mice in the syn-NICD-OE group. **D** DAPT in the mPFC induced increased $GABA_{B1}$ receptor mRNA levels in the mPFC of MIP mice [Two-way ANOVA followed by LSD test, main effect of DAPT, $F_{(1, 20)} = 17.38$, $P < 0.01$; main effect of METH, $F_{(1, 20)} = 9.88$, $P < 0.01$; DAPT × METH, $P > 0.05$]. **G** The co-localization of $GABA_{B1}$ receptor (Green) and Notch1 receptor (Red) were observed in the mPFC of native mice by double-label immunofluorescence staining assay. The areas in the rectangles were enlarged respectively in the bottom of the image. Arrows indicate expressed both receptors, and the scale bar represent 50 μm (images in the first row) and 20 μm (images in the second row). *$P < 0.05$, **$P < 0.01$ vs. control saline group. #$P < 0.05$, ##$P < 0.01$, ###$P < 0.001$ vs. paired METH group. The results are expressed as the mean ± SEM, $n = 6–7$.

METH sensitization. This phenomenon was similar to the results in previous studies. For example, Leos *et al*. have reported significant changes in the D1R and D2R mRNA expression in METH-acute and METH-sensitized groups [54]. Despite both D1R and D2R playing essential roles in acute METH exposure and METH sensitization, there was also no difference between the METH-acute group and the METH-sensitized group. In addition, the activity-regulated cytoskeleton-associated protein (Arc) gene encodes a cytoskeleton protein that regulates the neural networks of METH-acute-induced hyperactivity and behavioural sensitization [55]. The mRNA level of *Arc* gene in the METH-sensitized group also increased after acute METH administration in the mPFC [56]. Therefore, we hypothesized that the steady decreasing trend in Notch1 signaling after METH treatment may lead to sustained changes in synaptic plasticity in behavioural sensitization, although the mRNA levels of Notch1 signaling in the METH-acute and METH-sensitive groups did not change in the present study. This inference was further warranted by the increased level of $GABA_{B1}$ receptor in the METH-sensitized group compared with the METH-acute group, which also was supported by the results that the mRNA and protein levels of $GABA_{B1}$ receptor increased with decreased Notch1 signalling in the mPFC of mice.

Along with the behaviour sensitization, downregulation of neural Notch1 in the mPFC attenuates other MIP-related behaviours and overexpression of neural Notch1 aggravates other MIP-related behaviours (including anxiety-like behaviours, depression-like behaviours, social interaction and cognitive impairment). Consistent with our results, the administration of the DAPT in the mPFC alleviated cognitive deficits in a rat model of autism [57]. NaHS caused remission from the depression- and anxiety-like behaviours induced by type 1 diabetes mellitus by decreasing Notch1 signalling [58]. All of these results suggested that Notch1 signalling in the mPFC may play an important role in MIP and that the reduction in Notch1 signalling could be a protective factor against MIP.

Reduced activity of the GABAergic inhibitory network was one of the key factors in the occurrence of MIP [2, 59]. It has been reported that the activity of the GABAergic system in the mPFC decreased in METH-sensitized mice [27, 60]. Our results further confirmed the significant downregulation of GABA receptors and transporters in the mPFC of METH-sensitized mice. Interestingly, through a variety of GABA receptors and transporters expression analyses, we found that Notch1 signalling could negatively regulate $GABA_{B1}$ receptor expression. Furthermore, our results revealed that inhibition of Hes1, a transcriptional repressor of Notch1 signalling, could increase $GABA_{B1}$ receptor expression. Indeed, using ChIP-qPCR assays, we obtained evidence that the downstream transcriptional repressor Hes1 could directly bind to the $GABA_{B1}$ receptor promoters.

$GABA_{B1}$, a subunit of $GABA_B$ receptors, is responsible for G-protein coupling and modulates potassium channels and high-voltage calcium channels [61]. Activation of the $GABA_B$ receptor could reduce neuronal excitability [62] and exert an antipsychotic-like action in SCZ [63]. In addition, increasing $GABA_B$ receptor activity in the mPFC could decrease psychostimulant-induced dopamine levels in the prefrontal cortex [64] and ameliorate METH-induced locomotor activity [65] and cognitive deficits [66]. In accordance with these studies, increased $GABA_{B1}$ receptor expression in the mPFC induced by Notch1 signalling suppressed METH-induced locomotor hyperactivity, while decreased $GABA_{B1}$ receptor expression augmented the response to METH-induced locomotor activity. Furthermore, in vivo fiber photometry data suggest that the Notch1-shRNA-induced increase in $GABA_{B1}$ receptor may cause the inhibition of mPFC neurons. More notably, pretreatment with a $GABA_B$ receptor antagonist or agonist dramatically reversed the Notch1-induced changes in METH sensitization. Given the above, our results suggested that METH-induced decreases in mRNA and protein levels of Notch1 in the mPFC may increase $GABA_{B1}$ receptor expression and consequently inhibit mPFC activity, resulting in antipsychotic effects on the MIP-related behaviours (Fig. 6F). Although both $GABA_{B1}$ receptor and Notch1 signalling were significantly reduced in the mPFC of sensitized mice, this phenomenon may be resulting from direct METH influence or other transcription regulators. For example, glutamate can lead to rapid downregulation of $GABA_B$ receptors via lysosomal degradation in cortical neurons [67]. The higher levels of extracellular glutamate in mPFC of METH-acute [68] and METH-sensitized mice [69] may directly result in the downregulation of $GABA_{B1}$ receptor rather than Notch1 signalling.

A few interesting questions remain open following this study. First, the type of neuron on which the Notch1-Hes1-$GABA_{B1}$ pathway acts in the mPFC is still unknown. According to our results and previous studies [70], upregulation of the $GABA_{B1}$ receptor would lead to reduced mPFC activity. Thus, expression changes are most likely to occur in glutamatergic pyramidal neurons. Further investigations should be carried out to test this speculation. Second, the neuronal activity could be detected more precisely through electrophysiology, which could determine whether $GABA_{B1}$ expression changes in the presynaptic or postsynaptic cells. Finally, it would be worthwhile to identify the brain regions to which the activated mPFC neurons project in METH sensitization.

In conclusion, our study provides the first preliminary evidence to demonstrate reduced mRNA and protein levels of the

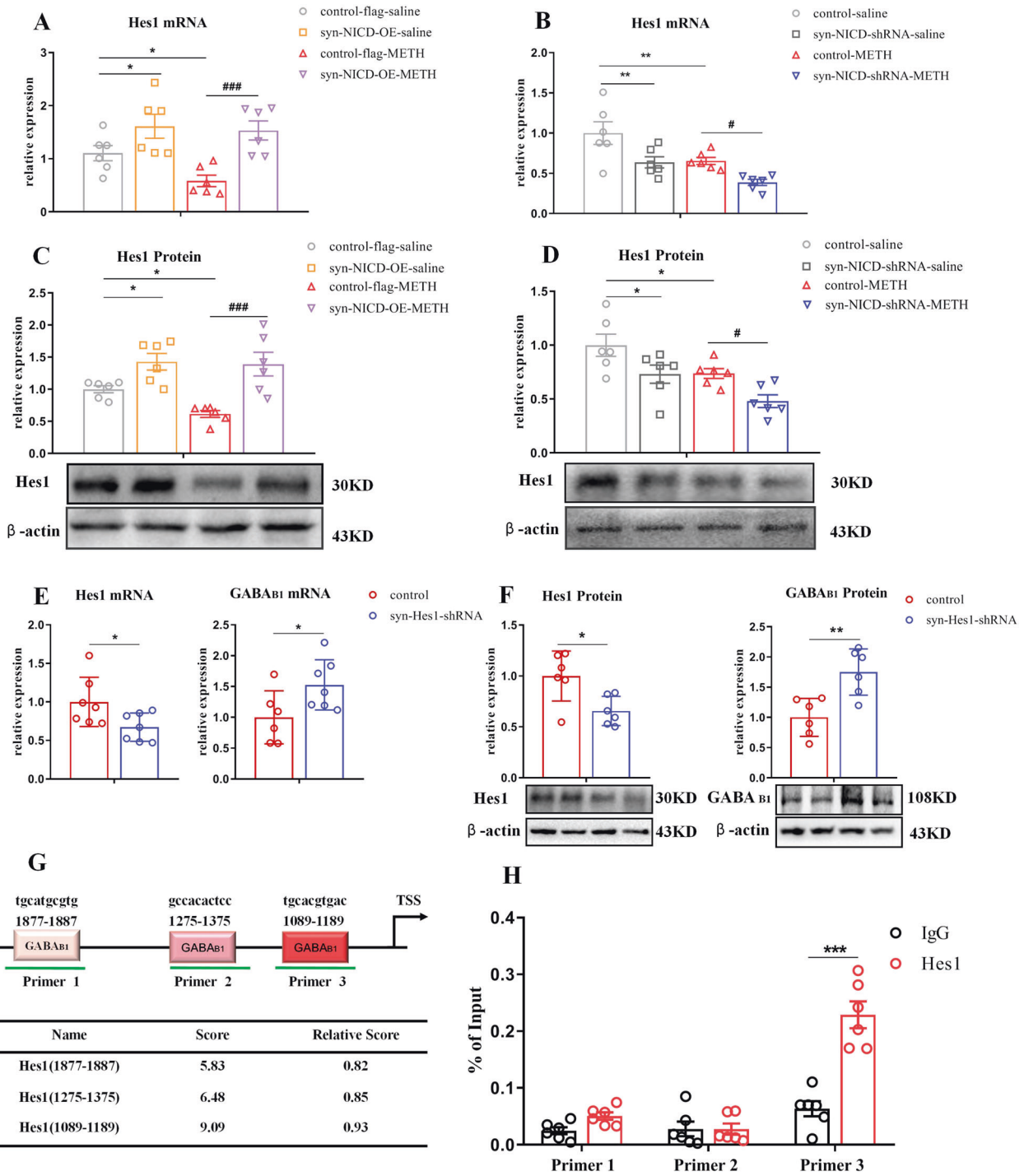

Fig. 5 The Notch1 signalling pathway regulated the $GABA_{B1}$ receptor via hes1. A–D Hes1 expression changes following regulation of the Notch1 signalling pathway in the mPFC of MIP mice by Two-way ANOVA followed by LSD test. Hes1 mRNA [**A** main effect of AAV, $F_{(1, 20)} = 17.47$, $P < 0.001$; METH, $F_{(1, 20)} = 2.89$, $P > 0.05$; AAV × METH, $P > 0.05$] and protein [**C** main effect of AAV, $F_{(1, 20)} = 25.73$, $P < 0.05$; METH, $F_{(1, 20)} = 3.16$, $P > 0.05$; AAV × METH, $P > 0.05$] levels were increased in the syn-NICD-OE group of mice. Hes1 mRNA [**B**, main effect of AAV, $F_{(1, 20)} = 14.17$, $P < 0.01$; METH, $F_{(1, 20)} = 12.56$, $P < 0.01$; AAV × METH, $P > 0.05$] and protein [**D**, main effect of AAV, $F_{(1, 20)} = 11.84$, $P < 0.01$; METH, $F_{(1, 20)} = 11.27$, $P < 0.01$; AAV × METH, $P > 0.05$] levels were decreased in the syn-NICD-shRNA group of mice. **E**, **F** Hes1 mRNA ($t_{12} = 2.35$, $^{*}P < 0.05$) and protein ($t_{10} = 2.95$, $^{*}P < 0.05$) levels were significantly lower in syn-Hes1-shRNA mice than control mice by student's *t* test. $GABA_{B1}$ receptor mRNA ($t_{11} = -2.27$, $^{*}P < 0.05$) and protein ($t_{10} = -3.71$, $^{**}P < 0.01$) levels were increased in the syn-Hes1-shRNA group by student's *t* test. **G**, **H**. The results of ChIP-qPCR assays indicated that Hes1 bound to the promoter of the $GABA_{B1}$ receptor. **G** Schematic diagram and table of the $GABA_{B1}$ promoter region showing potential binding sites of Hes1 predicted by the JASPAR database. **H** The naive mice mPFC were subjected to ChIP assay. Three paired primers were designed near the predicted binding sites of Hes1. ChIP-qPCR assays verified the association of Hes1 and the promoter of the $GABA_{B1}$ gene (Primer 3, $t_{10} = -6.11$, $^{***}P < 0.001$) by student's *t* test. $^{*}P < 0.05$, $^{**}P < 0.01$, $^{***}P < 0.001$ vs. control saline group. $\#P < 0.05$, $\#\#\#P < 0.001$ vs. paired METH group. The results are expressed as the mean ± SEM, $n = 6$–7.

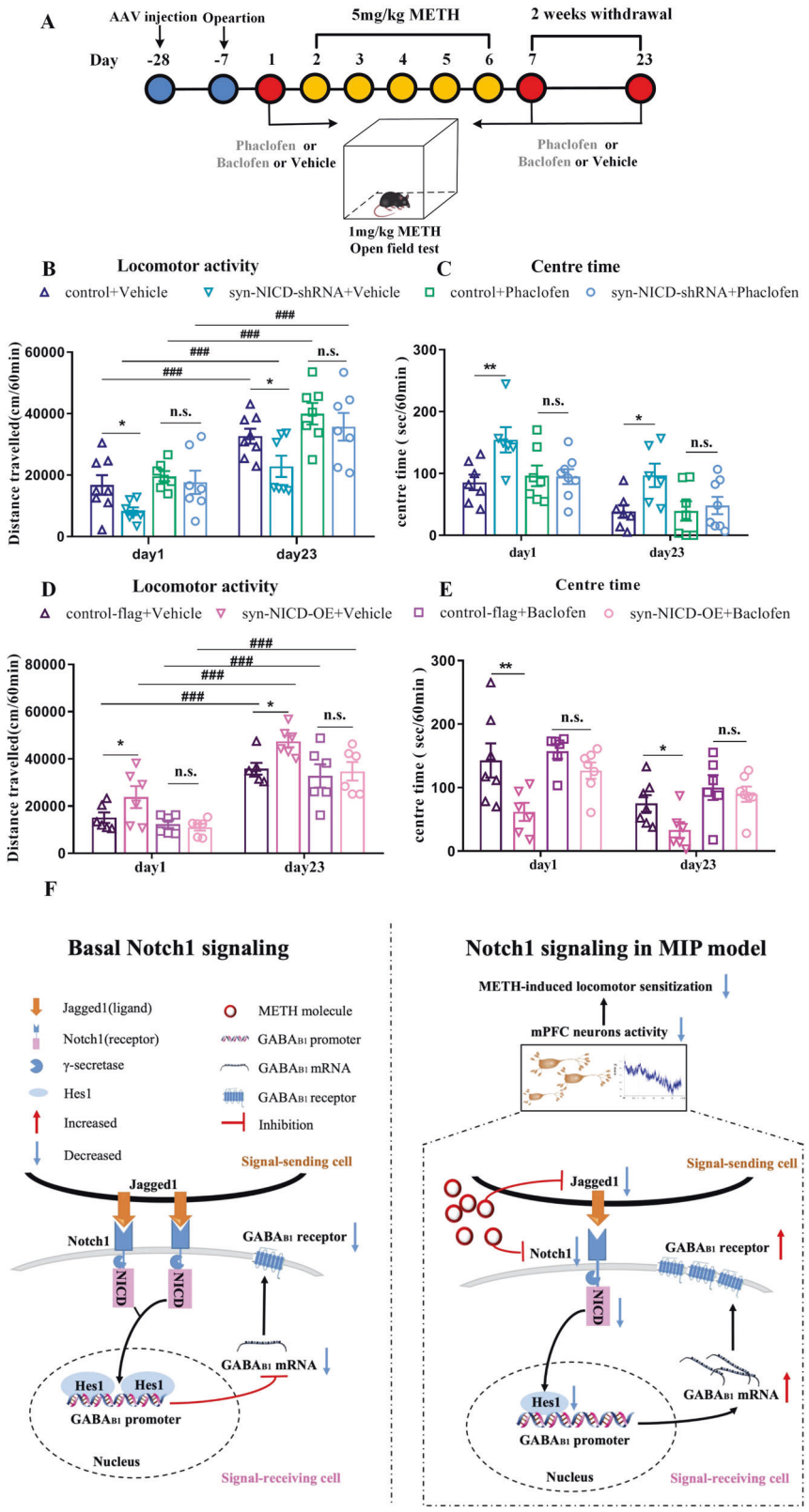

Notch1 signalling pathway in the mPFC of METH-induced locomotor sensitization. More importantly, the decreased Notch1 signalling in the mPFC of mice was capable of attenuating sensitization and other MIP-related behaviours. These effects can occur through increased $GABA_{B1}$ receptor expression as a result of Notch1-Hes1 signalling, which could inhibit mPFC neuronal activity (Fig. 6F). Our work proposes an important associations between Notch1 signalling and MIP-related neural plasticity. These findings will provide mechanistic insights into understanding of MIP and, ultimately, facilitate the development of new therapies for MIP.

Fig. 6 $GABA_B$ receptor antagonist (phaclofen) or agonist (baclofen) reversed the effect of Notch1 signalling in METH-induced sensitization. A Timeline of phaclofen or baclofen pretreatment for the syn-NICD-shRNA or syn-NICD-OE METH group in the locomotor activity test. **B**, **C** Phaclofen pretreatment reversed the significant decrease in locomotion and increase in centre time evoked by inhibition of NICD in the mPFC on day 1 and day 23. **B** Mixed-design ANOVA followed by post hoc multiple LSD test showed significant main effects of phaclofen [$F_{(1,\ 23)} = 17.61$, $P < 0.001$]; AAV [$F_{(1,\ 23)} = 5.10$, $P < 0.05$]; and AAV × phaclofen [$F_{(1,\ 23)} = 4.06$, $P < 0.05$] on locomotor activity. **C** Mixed-design ANOVA followed by post hoc multiple LSD test showed the significant main effect of phaclofen [$F_{(1,\ 24)} = 8.52$, $P < 0.01$]; AAV [$F_{(1,\ 24)} = 4.84$, $P < 0.05$]; and AAV×phaclofen [$F_{(1,\ 24)} = 7.61$, $P < 0.05$] on centre time. **D**, **E** Baclofen pretreatment reversed the significant increase in locomotion and decrease in centre time evoked by overexpression of NICD in the mPFC on day 1 and day 23. 6D. Mixed-design ANOVA with LSD post hoc multiple comparison was performed. There were significant main effects of baclofen [$F_{(1,\ 20)} = 11.31$, $P < 0.01$]; AAV [$F_{(1,\ 20)} = 5.11$, $P < 0.05$]; and AAV × baclofen [$F_{(1,\ 20)} = 4.34$, $P < 0.05$] on locomotor activity. **E** Mixed-design ANOVA followed by post hoc multiple LSD test showed significant main effect of baclofen [$F_{(1,\ 22)} = 11.46$, $P < 0.01$]; AAV [$F_{(1,\ 22)} = 11.12$, $P < 0.01$]; but not the AAV × baclofen [$F_{(1,\ 22)} = 2.86$, $P > 0.05$] on centre time. $^*P < 0.05$, $^{**}P < 0.01$ vs. the vehicle control group. $^{\#\#\#}P < 0.001$ vs. the same group on day1. n.s. means no significant changes. The results are expressed as the mean ± SEM, $n = 6$–8. **F** Working model of Notch1 signalling pathway–mediated regulation of the $GABA_{B1}$ receptor as a protective factor against METH-induced behaviour sensitization. We show that the baseline levels of Notch1 signalling in the mPFC as a consequence of ligand (Jagged1) and receptor (Notch1) interaction maintain the status quo of the baseline state (left). In the MIP model, Notch1 signalling downregulation in the mPFC results in an increase in the $GABA_{B1}$ receptor, thereby creating an environment that attenuates mPFC neural activity and METH-induced locomotor sensitization.

REFERENCES

1. Richards JR, Laurin EG. *Methamphetamine Toxicity*. StatPearls Publishing: Treasure Island, 2022.
2. Hsieh JH, Stein DJ, Howells FM. The neurobiology of methamphetamine induced psychosis. Front Hum Neurosci. 2014;8:537.
3. Grant KM, LeVan TD, Wells SM, Li M, Stoltenberg SF, Gendelman HE, et al. Methamphetamine-associated psychosis. J Neuroimmune Pharm. 2012;7:113–39.
4. Wearne TA, Cornish JL. A comparison of methamphetamine-induced psychosis and schizophrenia: a review of positive, negative, and cognitive symptomatology. Front Psychiatry. 2018;9:491.
5. Deng X, Huang Z, Li X, Li Y, Wang Y, Wu D, et al. Long-term follow-up of patients treated for psychotic symptoms that persist after stopping illicit drug use. Shanghai Arch Psychiatry. 2012;24:271–8.
6. Ujike H. Stimulant-induced psychosis and schizophrenia: the role of sensitization. Curr Psychiatry Rep. 2002;4:177–84.
7. Sato M, Chen CC, Akiyama K, Otsuki S. Acute exacerbation of paranoid psychotic state after long-term abstinence in patients with previous methamphetamine psychosis. Biol Psychiatry. 1983;18:429–40.
8. Akiyama K, Saito A, Shimoda K. Chronic methamphetamine psychosis after long-term abstinence in Japanese incarcerated patients. Am J Addict. 2011;20:240–9.
9. Dai H, Okuda H, Iwabuchi K, Sakurai E, Chen Z, Kato M, et al. Social isolation stress significantly enhanced the disruption of prepulse inhibition in mice repeatedly treated with methamphetamine. Ann N. Y Acad Sci. 2004;1025:257–66.
10. Janetsian SS, Linsenbardt DN, Lapish CC. Memory impairment and alterations in prefrontal cortex gamma band activity following methamphetamine sensitization. Psychopharmacol (Berl). 2015;232:2083–95.
11. Jaehne EJ, Ameti D, Paiva T, van den Buuse M. Investigating the role of serotonin in methamphetamine psychosis: unaltered behavioral effects of chronic methamphetamine in 5-HT(1A) knockout mice. Front Psychiatry. 2017;8:61.
12. Jing L, Liu B, Zhang M, Liang JH. Involvement of dopamine D2 receptor in a single methamphetamine-induced behavioral sensitization in C57BL/6J mice. Neurosci Lett. 2018;681:87–92.
13. Wearne TA, Mirzaei M, Franklin JL, Goodchild AK, Haynes PA, Cornish JL. Methamphetamine-induced sensitization is associated with alterations to the proteome of the prefrontal cortex: implications for the maintenance of psychotic disorders. J Proteome Res. 2015;14:397–410.
14. Greening DW, Notaras M. Chronic methamphetamine interacts with BDNF Val66Met to remodel psychosis pathways in the mesocorticolimbic proteome. Mol Psychiatry. 2021;26:4431–47.
15. Forrest AD, Coto CA, Siegel SJ. Animal models of psychosis: current state and future directions. Curr Behav Neurosci Rep. 2014;1:100–16.
16. Ables JL, Breunig JJ, Eisch AJ, Rakic P. Not(ch) just development: Notch signalling in the adult brain. Nat Rev Neurosci. 2011;12:269–83.
17. Siebel C, Lendahl U. Notch signaling in development, tissue homeostasis, and disease. Physiol Rev. 2017;97:1235–94.
18. Alberi L, Hoey SE, Brai E, Scotti AL, Marathe S. Notch signaling in the brain: in good and bad times. Ageing Res Rev. 2013;12:801–14.
19. Zhang X, Yang C, Gao J, Yin H, Zhang H, Zhang T, et al. Voluntary running-enhanced synaptic plasticity, learning and memory are mediated by Notch1 signal pathway in C57BL mice. Brain Struct Funct. 2018;223:749–67.
20. Howells FM, Uhlmann A, Temmingh H, Sinclair H, Meintjes E, Wilson D, et al. (1)H-magnetic resonance spectroscopy ((1)H-MRS) in methamphetamine dependence and methamphetamine induced psychosis. Schizophr Res. 2014;153:122–8.
21. Gan H, Zhao Y, Jiang H, Zhu Y, Chen T, Tan H, et al. A research of methamphetamine induced psychosis in 1,430 individuals with methamphetamine use disorder: clinical features and possible risk factors. Front Psychiatry. 2018;9:551.
22. Pietersen CY, Mauney SA, Kim SS, Passeri E, Lim MP, Rooney RJ, et al. Molecular profiles of parvalbumin-immunoreactive neurons in the superior temporal cortex in schizophrenia. J Neurogenet. 2014;28:70–85.
23. Wang HN, Liu GH, Zhang RG, Xue F, Wu D, Chen YC, et al. Quetiapine ameliorates schizophrenia-like behaviors and protects myelin integrity in cuprizone intoxicated mice: the involvement of notch signaling pathway. Int J Neuropsychopharmacol. 2015;19:pyv088.
24. Steine IM, Zayats T, Stansberg C, Pallesen S, Mrdalj J, Håvik B, et al. Implication of NOTCH1 gene in susceptibility to anxiety and depression among sexual abuse victims. Transl Psychiatry. 2016;6:e977.
25. Wearne TA, Parker LM, Franklin JL, Goodchild AK, Cornish JL. GABAergic mRNA expression is differentially expressed across the prelimbic and orbitofrontal cortices of rats sensitized to methamphetamine: Relevance to psychosis. Neuropharmacology. 2016;111:107–18.
26. Zhang X, Lee TH, Xiong X, Chen Q, Davidson C, Wetsel WC, et al. Methamphetamine induces long-term changes in GABAA receptor alpha2 subunit and GAD67 expression. Biochem Biophys Res Commun. 2006;351:300–5.
27. Bu Q, Lv L, Yan G, Deng P, Wang Y, Zhou J, et al. NMR-based metabonomic in hippocampus, nucleus accumbens and prefrontal cortex of methamphetamine-sensitized rats. Neurotoxicology. 2013;36:17–23.
28. Li Q, Zhang X, Cheng N, Yang C, Zhang T. Notch1 knockdown disturbed neural oscillations in the hippocampus of C57BL mice. Prog Neuropsychopharmacol Biol Psychiatry. 2018;84:63–70.
29. Liu S, Wang Y, Worley PF, Mattson MP, Gaiano N. The canonical Notch pathway effector RBP-J regulates neuronal plasticity and expression of GABA transporters in hippocampal networks. Hippocampus. 2015;25:670–8.
30. Xiu Y, Kong XR, Zhang L, Qiu X, Chao FL, Peng C, et al. White matter injuries induced by MK-801 in a mouse model of schizophrenia based on NMDA antagonism. Anat Rec (Hoboken). 2014;297:1498–507.
31. Duan H, Shen F, Li L, Tu Z, Chen P, Chen P, et al. Activation of the Notch signaling pathway in the anterior cingulate cortex is involved in the pathological process of neuropathic pain. Pain. 2021;162:263–74.
32. Sun K, Mu Q, Chang H, Zhang C, Wang Y, Rong S, et al. Postretrieval Microinjection of Baclofen Into the Agranular Insular Cortex Inhibits Morphine-Induced CPP by Disrupting Reconsolidation. Front Pharm. 2020;11:743.
33. Araki R, Hiraki Y, Nishida S, Kuramoto N, Matsumoto K, Yabe T. Epigenetic regulation of dorsal raphe GABA(B1a) associated with isolation-induced abnormal responses to social stimulation in mice. Neuropharmacology. 2016;101:1–12.
34. Vahid-Ansari F, Lagace DC, Albert PR. Persistent post-stroke depression in mice following unilateral medial prefrontal cortical stroke. Transl Psychiatry. 2016;6:e863.
35. Lammel S, Lim BK, Ran C, Huang KW, Betley MJ, Tye KM, et al. Input-specific control of reward and aversion in the ventral tegmental area. Nature. 2012;491:212–7.
36. Heredia L, Torrente M, Colomina MT, Domingo JL. Assessing anxiety in C57BL/6J mice: a pharmacological characterization of the open-field and light/dark tests. J Pharm Toxicol Methods. 2014;69:108–14.
37. Liu D, Liang M, Zhu L, Zhou TT, Wang Y, Wang R, et al. Potential Ago2/miR-3068-5p cascades in the nucleus accumbens contribute to methamphetamine-induced locomotor sensitization of mice. Front Pharm. 2021;12:708034.
38. Yu CH, Hsieh YS, Chen PN, Chen JR, Kuo DY. Knockdown of the transcript of ERK in the brain modulates hypothalamic neuropeptide-mediated appetite control in amphetamine-treated rats. Br J Pharm. 2018;175:726–39.
39. Zan GY, Wang YJ, Li XP, Fang JF, Yao SY, Du JY, et al. Amygdalar κ-opioid receptor-dependent upregulating glutamate transporter 1 mediates depressive-like behaviors of opioid abstinence. Cell Rep. 2021;37:109913.

40. Gandal MJ. Transcriptome-wide isoform-level dysregulation in ASD, schizophrenia, and bipolar disorder. Science. 2018;362:eaat8127.
41. Voce A, Calabria B, Burns R, Castle D, McKetin R. A systematic review of the symptom profile and course of methamphetamine-associated psychosis (substance use and misuse). Subst Use Misuse. 2019;54:549–59.
42. Okada N, Takahashi K, Nishimura Y, Koike S, Ishii-Takahashi A, Sakakibara E, et al. Characterizing prefrontal cortical activity during inhibition task in methamphetamine-associated psychosis versus schizophrenia: a multi-channel near-infrared spectroscopy study. Addict Biol. 2016;21:489–503.
43. Wearne TA, Parker LM, Franklin JL, Goodchild AK, Cornish JL. GABAergic mRNA expression is upregulated in the prefrontal cortex of rats sensitized to methamphetamine. Behav Brain Res. 2016;297:224–30.
44. Sorkaç A, Dilorio MA, O'Hern PJ, Baskoylu SN, Graham HK, Hart AC. LIN-12/Notch Regulates GABA Signaling at the Caenorhabditis elegans Neuromuscular Junction. G3 (Bethesda). 2018;8:2825–32.
45. Kabos P, Kabosova A, Neuman T. Blocking HES1 expression initiates GABAergic differentiation and induces the expression of p21(CIP1/WAF1) in human neural stem cells. J Biol Chem. 2002;277:8763–6.
46. Shin EJ, Dang DK, Tran TV, Tran HQ, Jeong JH, Nah SY, et al. Current understanding of methamphetamine-associated dopaminergic neurodegeneration and psychotoxic behaviors. Arch Pharm Res. 2017;40:403–28.
47. López-Gil X, Artigas F, Adell A. Role of different monoamine receptors controlling MK-801-induced release of serotonin and glutamate in the medial prefrontal cortex: relevance for antipsychotic action. Int J Neuropsychopharmacol. 2009;12:487–99.
48. Tanaka T, Ago Y, Umehara C, Imoto E, Hasebe S, Hashimoto H, et al. Role of prefrontal serotonergic and dopaminergic systems in encounter-induced hyperactivity in methamphetamine-sensitized mice. Int J Neuropsychopharmacol. 2017;20:410–21.
49. Ago Y, Tanaka T, Kita Y, Tokumoto H, Takuma K, Matsuda T. Lithium attenuates methamphetamine-induced hyperlocomotion and behavioral sensitization via modulation of prefrontal monoamine release. Neuropharmacology. 2012;62:1634–9.
50. Yang PP, Huang EY, Yeh GC, Tao PL. Co-administration of dextromethorphan with methamphetamine attenuates methamphetamine-induced rewarding and behavioral sensitization. J Biomed Sci. 2006;13:695–702.
51. Fatima M, Ahmad MH, Srivastav S, Rizvi MA, Mondal AC. A selective D2 dopamine receptor agonist alleviates depression through up-regulation of tyrosine hydroxylase and increased neurogenesis in hippocampus of the prenatally stressed rats. Neurochem Int. 2020;136:104730.
52. Toritsuka M, Kimoto S, Muraki K, Kitagawa M. Regulation of striatal dopamine responsiveness by Notch/RBP-J signaling. Transl Psychiatry. 2017;7:e1049.
53. Petruccelli E, Feyder M, Ledru N, Jaques Y, Anderson E, Kaun KR. Alcohol activates Scabrous-Notch to influence associated memories. Neuron. 2018;100:1209–23. e1204
54. Landa L, Jurajda M, Sulcova A. Altered dopamine D1 and D2 receptor mRNA expression in mesencephalon from mice exposed to repeated treatments with methamphetamine and cannabinoid CB1 agonist methanandamide. Neuro Endocrinol Lett. 2012;33:446–52.
55. Ujike H, Takaki M, Kodama M, Kuroda S. Gene expression related to synaptogenesis, neuritogenesis, and MAP kinase in behavioral sensitization to psychostimulants. Ann N. Y Acad Sci. 2002;965:55–67.
56. Kodama M, Akiyama K, Ujike H, Shimizu Y, Tanaka Y, Kuroda S. A robust increase in expression of arc gene, an effector immediate early gene, in the rat brain after acute and chronic methamphetamine administration. Brain Res. 1998;796:273–83.
57. Zhang Y, Xiang Z, Jia Y, He X, Wang L, Cui W. The Notch signaling pathway inhibitor Dapt alleviates autism-like behavior, autophagy and dendritic spine density abnormalities in a valproic acid-induced animal model of autism. Prog Neuropsychopharmacol Biol Psychiatry. 2019;94:109644.
58. Wang Y, Wang S, Xin Y, Zhang J, Wang S, Yang Z, et al. Hydrogen sulfide alleviates the anxiety-like and depressive-like behaviors of type 1 diabetic mice via inhibiting inflammation and ferroptosis. Life Sci. 2021;278:119551.
59. Brummelte S, Neddens J, Teuchert-Noodt G. Alteration in the GABAergic network of the prefrontal cortex in a potential animal model of psychosis. J Neural Transm (Vienna). 2007;114:539–47.
60. Peleg-Raibstein D, Knuesel I, Feldon J. Amphetamine sensitization in rats as an animal model of schizophrenia. Behav Brain Res. 2008;191:190–201.
61. Jacobson LH, Vlachou S, Slattery DA, Li X, Cryan JF. The gamma-aminobutyric acid B receptor in depression and reward. Biol Psychiatry. 2018;83:963–76.
62. Kohl MM, Paulsen O. The roles of GABAB receptors in cortical network activity. Adv Pharm. 2010;58:205–29.
63. Kantrowitz J, Citrome L, Javitt D. GABA(B) receptors, schizophrenia and sleep dysfunction: a review of the relationship and its potential clinical and therapeutic implications. CNS drugs. 2009;23:681–91.
64. Balla A, Nattini ME, Sershen H, Lajtha A, Dunlop DS, Javitt DC. GABAB/NMDA receptor interaction in the regulation of extracellular dopamine levels in rodent prefrontal cortex and striatum. Neuropharmacology. 2009;56:915–21.
65. Stafford AM, Reed C, Phillips TJ. Non-genetic factors that influence methamphetamine intake in a genetic model of differential methamphetamine consumption. Psychopharmacol (Berl). 2020;237:3315–36.
66. Wearne TA, Cornish JL. Inhibitory regulation of the prefrontal cortex following behavioral sensitization to amphetamine and/or methamphetamine psychostimulants: A review of GABAergic mechanisms. Prog Neuropsychopharmacol Biol Psychiatry. 2019;95:109681.
67. Maier PJ, Marin I, Grampp T, Sommer A, Benke D. Sustained glutamate receptor activation down-regulates GABAB receptors by shifting the balance from recycling to lysosomal degradation. J Biol Chem. 2010;285:35606–14.
68. Qi J, Han WY, Yang JY, Wang LH, Dong YX, Wang F, et al. Oxytocin regulates changes of extracellular glutamate and GABA levels induced by methamphetamine in the mouse brain. Addict Biol. 2012;17:758–69.
69. Lominac KD, Quadir SG, Barrett HM, McKenna CL, Schwartz LM, Ruiz PN, et al. Prefrontal glutamate correlates of methamphetamine sensitization and preference. Eur J Neurosci. 2016;43:689–702.
70. Hearing M, Kotecki L, Marron Fernandez de Velasco E, Fajardo-Serrano A, Chung HJ, Luján R, et al. Repeated cocaine weakens GABA(B)-Girk signaling in layer 5/6 pyramidal neurons in the prelimbic cortex. Neuron. 2013;80:159–17.

AUTHOR CONTRIBUTIONS

TN, FG and TC designed the project and provided materials. TN and LZ performed the cannulation, AAV microinjection and behaviour experiments. TN and SW performed the gene expression experiments, fiber photometry and CHIP. WZ, YX and YZ provide technical training necessary to perform the research. TN drafted the manuscript. TC, DM and HW provided critical revisions of the manuscript. All of the authors critically reviewed the content and approved the final version of the manuscript for publication.

FUNDING

This research was supported by grants from the National Natural Science Foundation of China (No. 82171879, No. 81772034, No. 81772033, No. 82171873, No. 81922024); Science, Technology and Innovation Commission of Shenzhen Municipality (RCJC20200714114556103).

COMPETING INTERESTS

The authors declare no competing interests.

ADDITIONAL INFORMATION

Supplementary information The online version contains supplementary material available at https://doi.org/10.1038/s41380-022-01662-z.

Correspondence and requests for materials should be addressed to Fanglin Guan or Teng Chen.

Reprints and permission information is available at http://www.nature.com/reprints

Publisher's note Springer Nature remains neutral with regard to jurisdictional claims in published maps and institutional affiliations.